

Chemical Shift Tensors in Peptides: A Quantum Mechanical Study

Ann E. Walling, Rica E. Pargas, and Angel C. de Dios*

Department of Chemistry, Georgetown University, 37th and O Streets, NW Washington, DC 20057

Received: June 2, 1997; In Final Form: July 23, 1997[⊗]

DFT-IGLO shielding tensor calculations for the non-hydrogen nuclei in model dipeptides are presented. The behavior of the principal components, their magnitude and orientation, is investigated as a function of the dihedral angles ϕ and ψ . For both C^o and amide N sites, the shielding tensor follows the molecular framework, while for C^α the tensor does not. Shielding tensor surfaces that span the entire Ramachandran surface ($\phi = -180^\circ$ to 180° , $\psi = -180^\circ$ to 180°) have been constructed for both carbonyl carbon and amide nitrogen shielding tensors in a model glycyl-glycine dipeptide. The principal tensor element σ_{22} of the carbonyl shielding tensor always lies close to the C=O bond (7° – 9°) while the σ_{11} component of the amide nitrogen shielding tensor is always slightly tilted (18° – 22°) from the N–H bond. The effects of hydrogen bonding on the orientation and magnitude of the shielding tensor components are also investigated at selected conformations: extended, $\phi = 180^\circ$ and $\psi = 180^\circ$; sheet, $\phi = -120^\circ$ and $\psi = 120^\circ$; and helix, $\phi = -60^\circ$ and $\psi = -60^\circ$. For C^α, calculations indicate that the shielding value along the C^α–H^α vector is very sensitive to secondary structure.

Introduction

Ab initio calculations of the nuclear magnetic shielding property of nuclei in peptides and proteins have become increasingly popular.¹ Most of these studies, however, have focused on the average or isotropic value of the NMR chemical shift. The chemical shift is a tensor quantity and is, therefore, capable of providing six independent pieces of information, namely, the magnitude and direction of each of the three principal components. Several papers on novel solid-state NMR techniques that offer the possibility of obtaining shielding tensor information in peptides and proteins have been published recently.^{2–9} The difficulty in designing experiments that will take advantage of all the information available from a shielding tensor is challenging. The magnitudes of each of the principal components can be readily obtained from a powder sample. To determine the principal axis system of a shielding tensor, single crystalline samples are normally required, however. Thus, it is probably not feasible to determine experimentally how the orientation of a shielding tensor for a given site in a polypeptide changes with the secondary structure.

The adequacy of present shielding computational methodologies in predicting not just the magnitude but also the orientation of the principal components has already been demonstrated in the case of the crystalline, zwitterionic L-threonine.¹⁰ Reasonable agreement is achieved for all the carbon sites, even in the presence of charged (–COO[–]) and polar groups (–OH). With this capability, it is now possible to probe theoretically the behavior of the shielding tensor, specifically, its orientation as a function of local structure and environment. Such information is very difficult to obtain empirically. At sites of high symmetry, it is possible to determine the orientation of the shielding tensor without doing any experiments or calculations. Systems of biological interest, such as peptides and proteins, often lack symmetry. Even if one assumes that the amide group in peptides is strictly planar, the orientation of only one of the principal tensor elements of the carbonyl carbon can be deduced from symmetry. The other two components that lie on the amide plane can be pointing at any direction in that plane. An

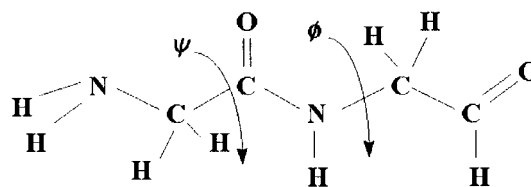
a priori knowledge of how the principal axis system of the shielding tensor depends on geometry will certainly be helpful in designing novel solid-state or even solution NMR experiments.

Protein secondary structure is encoded in the two dihedral angles, ϕ and ψ . The isotropic shielding and the values of the shielding components are sensitive not only to changes in these dihedral angles but also to minute changes in bond lengths and angles. On the other hand, the orientation of the principal components is more likely to be influenced by changes in geometry that involve large displacements. Therefore, it is very likely that studying shielding tensor orientations will present itself as a more direct monitor of dihedral angles in a peptide or protein.

Unlike experiments, theoretical calculations can also focus on one factor at a time. Shieldings in peptides can be influenced by either short-range or long-range factors. The effect of one dihedral angle can be studied separately. Hydrogen bonding can also be investigated. Such studies may not be possible experimentally, especially when most of the factors are normally simultaneously changing from one system to another. In this work, theoretical studies of how the shielding tensor components of the amide nitrogen, carbonyl carbon and, α carbon sites depend on the dihedral angles ϕ and ψ will be presented. This work is aimed at exploring trends that may be helpful in designing experiments that will fully utilize the information available from chemical shift measurements.

Computational Details

Calculations for the carbonyl carbon and amide nitrogen sites were performed using a model fragment:



The starting geometry was obtained from a geometry optimization.

[⊗] Abstract published in *Advance ACS Abstracts*, September 15, 1997.

TABLE 1: ^{13}C Shielding of Carbonyl Carbon in Glycyl-Glycine at Selected Conformations

ϕ (deg)	ψ (deg)	principal components (ppm)	direction cosines ^a		
			<i>x</i>	<i>y</i>	<i>z</i>
180	180	-73	0.0993	-0.9951	-0.0006
		18	0.9951	0.0993	0.0009
		83	-0.0008	-0.0006	1.0000
-120	120	-71	0.1190	-0.9917	-0.0482
		19	0.9926	0.1199	-0.0457
		87	0.0239	-0.0457	0.9987
-60	-60	-68	0.1090	-0.9940	0.0038
		16	0.9879	-0.1088	-0.0083
		88	-0.1106	-0.0083	0.9938

^a The *x*-axis is along the C=O bond, and the amide group CONH defines the *xy*-plane.

tion via molecular mechanics using the HyperChem program.¹¹ The dihedral angles were varied from $\phi = -180^\circ$ to 0° and $\psi = 180^\circ$ to 0° without modifying any of the optimized bond lengths or angles. Additional geometry optimizations were not performed since the primary aim of this work is to study the orientation of the principal components of the shielding tensor. The principal axis system of the shielding at any of the backbone nuclei should not be sensitive to minor changes in bond lengths and bond angles. An attenuated basis set was used: IGLO-III for the amide atoms (CONH) and an IGLO-II basis for the rest of the fragment.¹² Effects of hydrogen bond were investigated using a formamide molecule as the hydrogen bond partner. The shielding calculations were performed using the sum-over-states density functional perturbation theory (SOS-DFPT)¹³ implemented in the deMon-NMR code of Salahub et al.¹³⁻¹⁸ This particular method makes use of the individual gauge for localized orbitals (IGLO) method for the chemical shift computations.¹⁹ The exchange correlation functional employed was taken from Perdew and Wang²⁰ (PW91). These are the functionals recommended by the authors of the demon-NMR program.¹³ For the shielding computation of the C $^\alpha$ site, a model fragment containing alanine was used. In these calculations a uniform IGLO-II basis was used. Additional computations were also performed for model fragments; *N*-formyl-Ala-X-amide and *N*-formyl-X-Ala-amide, where X is any one of the naturally occurring amino acids, at the following representative conformations: extended, $\phi = 180^\circ$ and $\psi = 180^\circ$; sheet, $\phi = -120^\circ$ and $\psi = 120^\circ$; and helix, $\phi = -60^\circ$ and $\psi = -60^\circ$. These were performed to verify the trends observed in the smaller glycyl-glycine model compound. The full shielding tensor of a nucleus is an asymmetric tensor, and theory provides this. The symmetric part of this tensor is relevant to experiments, and all references to components of the shielding tensor in the remainder of this paper correspond to the symmetric part of the tensor.

Results and Discussion

C $^\circ$ Shielding Tensor. Table 1 shows results for the shielding calculations for the carbonyl carbon nucleus in three representative conformations: extended, $\phi = 180^\circ$ and $\psi = 180^\circ$; sheet, $\phi = -120^\circ$ and $\psi = 120^\circ$; and helix, $\phi = -60^\circ$ and $\psi = -60^\circ$. The direction cosines are given with respect to a molecular Cartesian frame which has the *x*-axis lying on the C=O bond and the *z*-axis being normal to the amide plane. Figure 1 displays a tensor plot for the C $^\circ$ shielding in the extended conformation. In this figure, the shielding tensor is represented by a Jorgensen-Salem plot.²¹ The distance of the contour surface from the nucleus of interest (in this case, C $^\circ$) in a given radial direction is proportional to the absolute shielding response

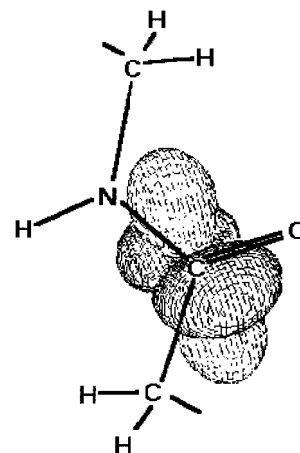


Figure 1. A tensor plot of the C $^\circ$ shielding for an extended conformation. The most shielded component (σ_{33}) is perpendicular to the amide plane; σ_{22} lies on the amide plane and is almost parallel to the C=O vector while σ_{11} is perpendicular to the C=O vector.

to an external magnetic field applied in that direction. The most shielded component (σ_{33}) in all three cases lies along the *z*-axis, perpendicular to the amide plane. The component that lies close to the C=O bond is σ_{22} . The least shielded component also lies on the amide plane and is perpendicular to the C=O bond. In all three cases, the orientation of the C $^\circ$ shielding tensor appears to follow the molecular framework. Upon inspection of the entire *Ramachandran* surface, the angle that σ_{22} makes with the C=O bond falls within the range 6° – 9° . Since the C $^\circ$ shielding tensor is intimately related to the amide plane and the C=O bond, the spatial relationship between the shielding tensor of C $^\circ$ in adjacent residues in a polypeptide or protein becomes a function of the dihedral angle ϕ . Thus, a 2D solid-state experiment that correlates two C $^\circ$ shielding tensors can be designed to determine this dihedral angle.

Hydrogen bond effects can be modeled by adding a formamide molecule in the computation. The atoms of the formamide molecule are placed on the same plane as the amide group of the dipeptide. A linear hydrogen bond is assumed for O \cdots H–N with a 120° angle for C=O \cdots H. Only one set of orientation and distance was used. The hydrogen bond distance O \cdots H is set at 2.0 Å. Upon inclusion of a formamide molecule as a hydrogen bond partner, the following changes in the C $^\circ$ shielding tensor occur. For the extended conformation, the most shielded component σ_{33} does not change appreciably (less than 1 ppm). The isotropic shielding goes down by about 2 ppm with hydrogen bonding, in agreement with a previous study.²² The least shielded component σ_{11} increases by 4 ppm in the presence of a formamide molecule while σ_{22} decreases by 10 ppm. A similar trend is observed for the other two conformations. The helical model shows, however, a greater hydrogen bond dependence; its isotropic value goes down by about 4 ppm since its σ_{22} element has become more sensitive. In this particular conformation, σ_{22} decreases by 14 ppm while σ_{11} goes up by only 2 ppm. The orientation of the principal components is not affected by hydrogen bonding in all three cases.

From the additional computations involving ala-X fragments where X is one of the naturally occurring amino acids, the same trends are observed. In all cases, the C $^\circ$ shielding tensor does follow the directions given by the amide plane and the C=O bond. Furthermore, for the X-ala fragments, the same scenario also exists. Thus, from the theoretical calculations, it can be concluded that the principal axis system of the C $^\circ$ shielding tensor for all amino acids is indeed intimately related to the amide plane and the direction of the C=O bond. In all cases,

TABLE 2: ^{15}N Shielding of Amide Nitrogen in Glycyl-Glycine at Selected Conformations

ϕ (deg)	ψ (deg)	principal components (ppm)	direction cosines ^a		
			<i>x</i>	<i>y</i>	<i>z</i>
180	180	38	0.9458	-0.3248	-0.0008
		164	0.0011	0.0007	1.0000
		228	0.3248	0.9458	-0.0011
-120	120	45	0.9491	-0.3149	-0.0087
		146	-0.0118	-0.0630	0.9979
		214	-0.3148	-0.9470	-0.0635
-60	-60	67	0.9248	-0.3683	-0.0957
		168	0.0033	-0.2437	0.9699
		215	-0.3805	-0.8972	-0.2241

^a The *x*-axis is along the N-H bond, and the amide group CONH defines the *xy*-plane.

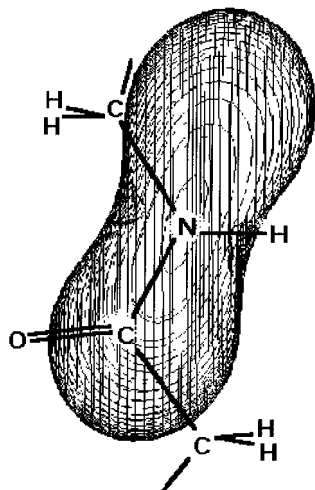


Figure 2. A tensor plot of the amide N shielding for an extended conformation. The least shielded component (σ_{11}) is tilted by 19° from the N-H bond; σ_{22} lies normal to the amide plane while the most shielded component lies on the amide plane and is about 80° from the N-H bond.

σ_{33} is found to be normal to the amide plane while σ_{22} lies almost parallel to the C=O bond.

Amide N Shielding Tensor. Table 2 shows results for the shielding calculations for the amide nitrogen nucleus in three representative conformations: extended, $\phi = 180^\circ$ and $\psi = 180^\circ$; sheet, $\phi = -120^\circ$ and $\psi = 120^\circ$; and helix, $\phi = -60^\circ$ and $\psi = -60^\circ$. The direction cosines are given with respect to a molecular Cartesian frame which has the *x*-axis lying along the N-H bond and the *z*-axis being normal to the amide plane. Figure 2 shows a tensor plot of the amide N shielding for the extended conformation. In all three cases, the component that lies along the *z*-axis is σ_{22} . The least shielded component, σ_{11} , lies on the amide plane and is tilted by about 18° – 22° from the N-H vector, in complete agreement with experiment.²³ The negative sign of the direction cosine with respect to the *y*-axis indicates that the tilting is toward the N-C^o vector, which likewise agrees with experiment.²³ The most shielded component, σ_{33} , becomes significantly tilted (about 13°) from the peptide plane in the helixlike conformer. In fact, a closer inspection of the whole Ramachandran surface reveals maximum departure (by as much as 45°) from the amide plane of the σ_{33} component at around $\psi_{i-1} = 30^\circ$. In this region, the σ_{22} component is no longer normal to the amide plane. In summary, for $\psi_{i-1} = -60^\circ$ to 60° , σ_{22} and σ_{33} begin to rotate about the axis of σ_{11} .

Thus, unlike the carbonyl carbon site, the orientation of the amide N shielding tensor does not strictly follow the amide molecular frame. Only in extended and sheet conformations

TABLE 3: the Amide H Shielding Tensor in Glycyl-Glycine (Extended Conformation), with and without Hydrogen Bonding

	principal components (ppm)	direction cosines ^a		
		<i>x</i>	<i>y</i>	<i>z</i>
without H-bonding	18.6	0.0009	0.0002	1.0000
	26.1	0.6971	-0.7170	-0.0005
	30.0	-0.7170	-0.6971	0.0008
with H-bonding	13.4	0.0006	0.0002	1.0000
	23.6	0.1657	-0.9862	0.0001
	30.3	-0.9862	-0.1657	0.0006

^a The *x*-axis is along the N-H bond, and the amide group CONH defines the *xy*-plane. A linear H-bond (N-H-O) is used with a 2.0 Å distance for N-O. An extended conformation is used.

does one component appear to be normal to the amide plane. With helical dihedral angles, a substantial deviation of the σ_{33} component from the amide plane is observed. Although the σ_{22} and σ_{33} components are no longer following the amide plane, the least shielded component σ_{11} remains close to the N-H bond. Therefore, one can still take advantage of this behavior. The spatial relationship between the least shielded component of N shielding tensors in adjacent residues in a polypeptide or protein is a function of the dihedral angle ψ .

From the additional computations involving X-ala fragments where X is one of the naturally occurring amino acids, a similar behavior for σ_{11} is observed. In all cases, the least shielded component of the alanine N shielding tensor always lies on the amide plane and is tilted by about 20° from the N-H vector. However, the deviation of σ_{22} from the normal to the amide plane becomes evident even in the extended conformation. For the nitrogen shielding tensor of the X residue in the ala-X model compounds, a situation similar to that of the alanine N shielding tensor is observed. In all three conformers of the other amino acids, σ_{11} is tilted from the N-H bond, and the deviation from the normal to the amide plane of the σ_{22} is more pronounced at the extended conformation. Thus, it appears that glycine is an exceptional case. The other amino acids indicate that their helical and sheet conformers have σ_{22} closer to being perpendicular to the amide plane.

In the presence of hydrogen bonding as represented by a formamide molecule whose O atom is 2.0 Å from the H of the amide N of interest (a linear hydrogen bond is also assumed), the isotropic shielding of the amide N nucleus goes down by 4–5 ppm in all three conformers. The behavior of each principal component is dependent, however, on the dihedral angles. In both extended and helical conformation, only σ_{11} and σ_{33} appear to be influenced by the presence of the formamide molecule. Both become deshielded by about 7–9 ppm. In the sheet conformer, all three components are affected with σ_{22} displaying a hydrogen-bond dependence of opposite sign. This component increases (by about 8 ppm) with hydrogen bonding, and since the change in the isotropic shielding is similar to those of the helical and extended conformers, both σ_{11} and σ_{33} of the N shielding tensor in the sheet model become deshielded by 9–12 ppm. As in C^o shielding, hydrogen bonding does not have a considerable effect on the orientation of the principal components of the amide N shielding tensor.

Amide H Shielding Tensor. In studying the shielding tensor of the amide proton, it is necessary to include hydrogen bonding. Without a hydrogen-bond partner, the orientation of the principal components is not well-defined with respect to the amide molecular framework. Only the orientation of the least shielded component, σ_{11} , directly relates to the molecular axis if hydrogen bonding is not present as shown in Table 3. The least shielded component, with or without hydrogen bonding, lies normal to

TABLE 4: Calculated C^α Shielding for Various Amino Acids in Model Peptides

amino acid	sheet model ($\phi = -120^\circ$, $\psi = -120^\circ$)		helix model ($\phi = -60^\circ$, $\psi = -60^\circ$)	
	isotropic shielding (ppm)	projection on $C^\alpha-H^\alpha$ vector (ppm)	isotropic shielding (ppm)	projection on $C^\alpha-H^\alpha$ vector (ppm)
Ala	138.3	117.9	132.1	135.2
Val	132.2	110.0	124.5	127.9
Asn	139.0	116.8	132.3	134.9
His	138.7	121.5	131.0	136.0
Lys	135.7	114.2	128.5	132.5
Ser	134.5	112.8	127.4	134.8
Gln	133.8	112.0	127.3	131.3
Trp	136.1	111.0	129.3	128.9
Thr	132.3	112.5	125.2	130.9
Arg	135.8	115.0	129.3	133.0
Phe	134.3	113.2	127.3	132.1
Cys	135.8	114.0	128.8	130.8
Leu	136.8	111.8	129.5	130.7
Tyr	134.2	112.8	127.4	131.5
Ile	131.8	111.3	124.2	129.4
Glu	130.8	107.6	125.0	128.2
Met	133.8	112.7	127.3	130.6
Asp	131.1	110.6	125.9	130.9

the amide plane. With hydrogen bonding, the most shielded component, σ_{33} , begins to align with the N-H vector. The principal axis system of the amide proton shielding obtained from the calculations in the presence of hydrogen bonding agrees with the experimentally observed orientation for *N*-acetylvaline from single-crystal work of Gerald et al.²⁴ It does not agree, however, with the more recent work of Wu et al.²³ on Ala-Leu. With Leu, the amide proton shielding components found experimentally to lie on the amide plane are σ_{11} and σ_{33} . Calculations involving an alanyl-leucine fragment do not agree with these experimental observations. From symmetry arguments, the component that is normal to the amide plane should be the least shielded component, σ_{11} , not σ_{22} . The calculated orientation in this paper agrees with symmetry arguments and the experimentally determined orientation of the principal components of the amide proton in *N*-acetylvaline.

α Carbon Shielding Tensor. Of all the sites in a protein, the shielding of the C^α nucleus seems to be the most tractable.²⁵ Even for this site, the error is still within 1 ppm, which translates to about 10% of the largest observed chemical shift range for C^α in proteins for a given amino acid. Thus, it may be useful to find a more sensitive piece of the chemical shift tensor that may have the same amount of error but a greater sensitivity to the secondary structure of the protein. Table 4 shows calculated shieldings for the C^α nuclei in various amino acids for the two conformations representative of their structure in proteins, helical and sheet. The isotropic shieldings and the value of the shielding tensor along the $C^\alpha-H^\alpha$ vector are presented for each case. Evidently, the results are consistent with the general observation that helical C^α sites are deshielded compared with those of sheet geometry.²⁶ Surprisingly, an opposite trend is seen when one looks at the projection of the C^α shielding tensor on the $C^\alpha-H^\alpha$ vector. For sheet residues, the least shielded component lies almost parallel to the N-H vector of the following residue. Incidentally, the $C^\alpha-H^\alpha$ bond has an orientation not exactly parallel but close to that of the N-H bond. Thus, the projection of the shielding tensor along the $C^\alpha-H^\alpha$ bond contains a large contribution from the least shielded component, σ_{11} . In helical residues, the least shielded component now lies almost normal to the amide plane, perpendicular to the N-H bond. The $C^\alpha-H^\alpha$ vector still lies close to the amide plane; thus, the contribution of the least

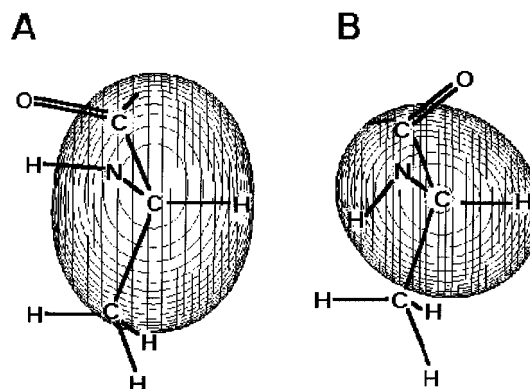


Figure 3. (A) A tensor plot of the C^α shielding in alanine with sheet dihedral angles ($\phi = -120^\circ$, $\psi = 120^\circ$). (B) Same as (A) but with helical dihedral angles ($\phi = -60^\circ$, $\psi = -60^\circ$).

shielded component to the projection of the C^α shielding tensor on the $C^\alpha-H^\alpha$ bond becomes minimal. As a result, the value of the shielding along the $C^\alpha-H^\alpha$ bond is now larger. Although the difference between the isotropic shieldings of helical and sheet C^α sites is only 5–8 ppm, the difference between the projection of the C^α shielding on the $C^\alpha-H^\alpha$ bond can be as large as 22 ppm. These differences become more evident when one compares the tensor plots of the C^α shielding in sheet and helical geometries as shown in Figure 3. In the sheet geometry (Figure 3A), it can be seen that the short axis of the shielding tensor coincides with the C-H vector while for a helical residue (Figure 3B), this is no longer true.

Conclusions

The calculated shielding tensors for sites in model peptides reveal the following interesting trends: (1) The principal axis system of the C° shielding tensor follows the directions given by the amide plane and the C=O bond. (2) Unlike the C° site, the shielding of the amide N appears not to follow strictly the molecular plane. (3) Hydrogen bonding does not have a considerable effect on the orientation of the principal axis system of both C° and amide N shielding tensors. (4) Hydrogen bonding defines the orientation of the principal axis system of the amide H shielding tensor. (5) The value of the C^α shielding along the $C^\alpha-H^\alpha$ bond is very sensitive to the dihedral angles ϕ and ψ . It is hoped that these theoretical results will help in the design of novel NMR experiments aimed at determining protein structures from chemical shift tensors.

Acknowledgment. This work was supported in part by a New Faculty Award from the Camille and Henry Dreyfus Foundation. Acknowledgment is made to the donors of the Petroleum Research Fund, administered by the American Chemical Society, for partial support of this research. The authors thank Professor D. R. Salahub for providing a copy of the demon-KS and the demon-NMR programs, Professor A. E. Hansen for providing PSI88, a tensor plotting program, and Professor C. J. Jameson and Dr. A. Bax for helpful discussions.

References and Notes

- de Dios, A. C. *Prog. NMR Spectrosc.* **1996**, *29*, 229.
- Raleigh, D. P.; Creuzet, F.; Das Gupta, S. K.; Levitt, M. H.; Griffin, R. G. *J. Am. Chem. Soc.* **1989**, *111*, 450.
- Pan, Y.; Gullion, T.; Schaefer, J. *J. Magn. Reson.* **1990**, *90*, 330.
- Weliky, D. P.; Dabbagh, G.; Tycko, R. *J. Magn. Reson. A* **1993**, *104*, 10.
- Nakai, T.; McDowell, C. A. *Chem. Phys. Lett.* **1994**, *217*, 234.
- Dabbagh, G.; Weliky, D. P.; Tycko, R. *Macromolecules* **1994**, *27*, 6183.

- (7) Tomita, Y.; O'Connor, E. J.; McDermott, A. *J. Am. Chem. Soc.* **1994**, *116*, 8766.
- (8) Schmidt-Rohr, K. *Macromolecules* **1996**, *29*, 3975.
- (9) Schmidt-Rohr, K. *J. Am. Chem. Soc.* **1996**, *118*, 7601.
- (10) de Dios, A. C.; Laws, D. D.; Oldfield, E. *J. Am. Chem. Soc.* **1994**, *116*, 7784.
- (11) *Hyperchem*; Hypercube, Inc.: Waterloo, Ontario.
- (12) Kutzelnigg, W.; Fleischer, U.; Schindler, M. *NMR: Basic Princ. Prog.* **1990**, *23*, 165.
- (13) Malkin, V. G.; Malkina, O. L.; Casida, M. E.; Salahub, D. R. *J. Am. Chem. Soc.* **1994**, *116*, 5898.
- (14) Salahub, D. R.; Fournier, R.; Mlynarski, P.; Papai, I.; St-Amant, A.; Ushio, J. In *Density Functional Methods in Chemistry*; Labanowski, J., Andzelm, J., Eds.; Springer: New York, 1991.
- (15) St-Amant, A.; Salahub, D. R. *Chem. Phys. Lett.* **1990**, *169*, 387.
- (16) St-Amant, A. Thesis, Université de Montréal, 1992.
- (17) Malkin, V. G.; Malkina, O. L.; Salahub, D. R. *Chem. Phys. Lett.* **1993**, *204*, 87.
- (18) Malkin, V. G.; Malkina, O. L.; Eriksson, L. A.; Salahub, D. R. In *Modern Density Functional Theory: A Tool for Chemistry; Theoretical and Computational Chemistry*; Seminario, J. M., Politzer, P., Eds.; Elsevier: Amsterdam, 1995; Vol. 2.
- (19) Kutzelnigg, W. *Isr. J. Chem.* **1980**, *19*, 193.
- (20) Perdew, J. P.; Wang, Y. *Phys. Rev. B* **1992**, *45*, 13244.
- (21) Hansen, A. E.; Bouman, T. D. *J. Chem. Phys.* **1989**, *91*, 3552.
- (22) de Dios, A. C.; Oldfield, E. *J. Am. Chem. Soc.* **1994**, *116*, 11485.
- (23) Wu, C. H.; Ramamoorthy, A.; Gierasch, L. M.; Opella, S. J. *J. Am. Chem. Soc.* **1995**, *117*, 6148.
- (24) Gerald, R.; Bernhard, T.; Haeberlen, U.; Rendell, J.; Opella, S. J. *J. Am. Chem. Soc.* **1993**, *115*, 777.
- (25) Le, H.; Pearson, J. G.; de Dios, A. C.; Oldfield, E. *J. Am. Chem. Soc.* **1995**, *117*, 3800.
- (26) Spera, S.; Bax, A. *J. Am. Chem. Soc.* **1991**, *113*, 5490.